

# Applying of PIV/PTV Methods for Physical Modeling of the Turbulent Buoyant Jets in a Stratified Fluid

Valery Bondur<sup>1</sup>, Yurii Grebenyuk<sup>1</sup>, Ekaterina Ezhova<sup>2</sup>,  
Alexander Kandaurov<sup>2</sup>, Daniil Sergeev<sup>2</sup> and Yuliya Troitskaya<sup>2</sup>

<sup>1</sup>AEROCOSMOS Institute for Scientific Research of Aerospace Monitoring

<sup>2</sup>Institute of Applied Physics Russian Academy of Sciences  
Russia

## 1. Introduction

Modern optical methods of flow visualization: Particle Tracking Velocimetry (PTV) and Particle Image Velocimetry (PIV) (see (Adrian, 1981)) are widely used in experimental investigations of air and liquid flows for scientific and industrial purposes. They are common in exploration of such processes as heat and mass transfer in power plants, flows in aircraft and shipbuilding, and medico-biological applications. Nowadays this technique is also employed in the laboratory modeling of geophysical flows (Sergeev & Troitskaya, 2011) including air-sea interaction (Reul et al., 1999; Veron et al., 2007); flows in water column and their interaction with bottom topography (Umeyama, 2008; Zhang et al., 2007); vortex flows (Beckers et al., 2002; Heist et al., 2003).

The present work is devoted to the investigation of the new class of flows by PIV/PTV-methods – oscillating buoyant jets (fountains) in stratified fluid. (Bondur & Grebenyuk, 2001; Bondur 2004, 2011; Bondur et al. 2006, 2009). Among the applications of these flows are heat and moisture exchange in the atmosphere and cloud formation (Turner, 1966). The investigation of buoyant jets in stratified fluid is extremely important for the development of new technologies of sewage disposal by coastal cities (Koh & Brooks, 1975). The end body of such systems is a submerged collector. A typical diffuser of a modern collector is a pipe with lots of outlets. Sewage water (which has almost the density of fresh water after sewage disposal plants) is discharged into ambient salt water to produce buoyant jets (Bondur, 2011; Bondur et al, 2006, 2009). One of the main questions when constructing diffusers of these collectors is a regime of jet flows when they are trapped by pycnocline and don't reach the surface.

Sewage disposal to the ocean is an example of the man's impact, influencing mass transfer, hydrodynamics, hydrobiology and coastal ecosystem state as a whole (Bondur, 2011). The complex investigation of these processes includes mathematic modeling of jets dynamics (Bondur, 2011; Bondur et al, 2006, 2009; Bondur & Grebenyuk, 2001; Koh & Brooks, 1975; Ozmidov 1986), contact methods (Bondur 2006; Bondur & Tsidilina, 2006; Gibson et al., 2006 a), and airborne and spaceborne remote sensing (Bondur, 2004, 2006, 2011; Bondur

&Grebenyuk, 2001). The investigation of physical mechanisms, responsible for surface manifestations of sewage flows, is a challenging problem. In the papers (Bondur, 2004, 2006, 2011; Bondur &Grebenyuk 2001) mechanisms, resulting from surface deformation by rising vortices or internal waves are suggested, and in works (Bondur et al., 2005; Gibson et al., 2006 b, 2007a,b) surface manifestations are explained by the complex interaction between turbulence, internal waves, tides and bottom topography.

The intensive generation of internal waves by buoyant jets from submerged wastewater outfalls in stratified fluid was investigated by contact methods in experiments on the laboratory scale modeling of these systems (Bondur et al, 2009, 2010 a, 2010 b; Troitskaya et al., 2008). However, in order to explore the possibility of internal waves manifestation and mechanisms of their generation by buoyant jets, the additional experiments were needed which allowed high-precision measurements of velocity fields of flows on the surface and in the water column. Contact sensors are not applicable for such systems since they cause essential perturbations in the investigated flow. Thus, in new experimental series non-invasive methods were employed, based on the flow visualization (modified PIV/PTV-methods), that allowed the effective solution to this problem.

The Chapter is organised as follows. The laboratory scale modeling of buoyant jets and the investigation of surface flows induced by these jets with the application of PIV-technique is described in Section 2. Section 3 is devoted to the testing of PIV-methods for the measurement of velocity fields in buoyant jets in stratified fluid. The last Section deals with the application of this method for the laboratory scale modeling. The parameters of oscillating jets are compared with the characteristics of internal waves. Special methods of video processing are employed to investigate the structure of jet perturbation modes.

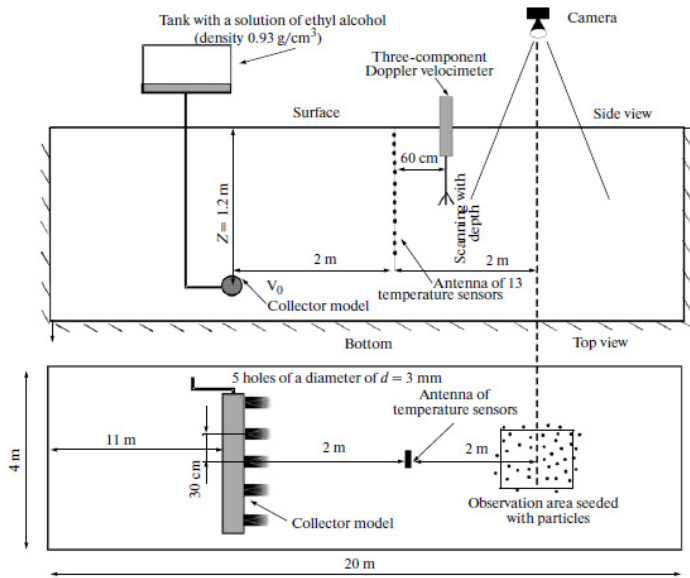
## **2. Experimental studies on measurements of the surface flows induced by submerged buoyant jets in the thermostratified tank with the modified PTV-method**

The main purpose of investigations, described in this part, is to assess the possibility of internal waves manifestation caused by a submerged sewer system on the sea surface. To solve this complicated problem it is necessary to obtain the properties of inhomogeneous flow fields created on the sea surface.

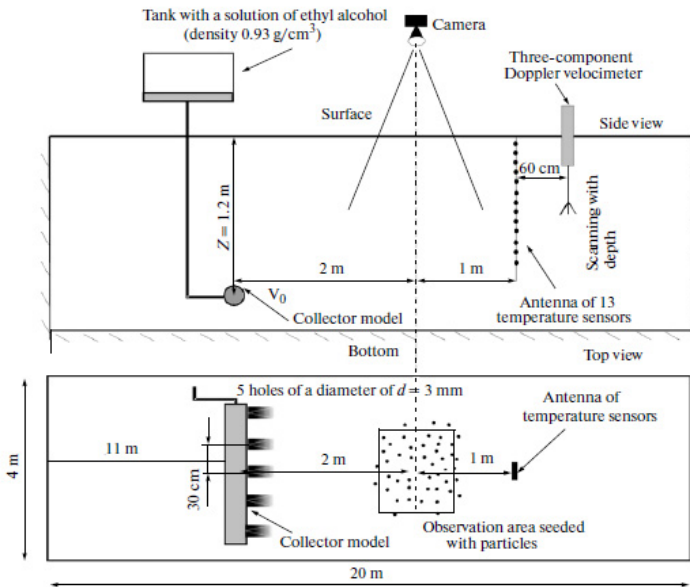
The experimental study of these processes was carried out on the basis of laboratory scale modeling at the Large Thermally Stratified Tank (LTST) of the Institute of Applied Physics, Russian Academy of Sciences (IAP RAS). The experiments included measurements in the water, and the main attention was drawn to the measurements of the surface flow, where the PTV- method was used.

### **2.1 Experimental setup for the scale laboratory modeling of the surface flows induced by the typical submerged sewer system in the LTST**

The principal scheme of experiments is shown in Fig1. The LTST dimensions are as follows: 20 m in length, 4 m in width, and 2 m in depth. The temperature (density) stratification in the LTST is generated through liquid heating and cooling with heat exchangers installed along the tank walls (Arabadzhi et al., 1999; Bondur et al., 2009). It results in the formation of the inhomogeneous vertical distribution of the temperature (density) in the tank.



(a)



(b)

Fig. 1. General scheme of LTST IAP RAS experiments with the location of temperature and velocity sensors before the area of surface PTV measurements series S1 - (a), and behind S2 - (b)

The experiments were carried out using distribution of temperature with shallow thermocline depth of 13–15 cm on the average (profile 1 in Fig.2), with the total water depth of 130 cm.

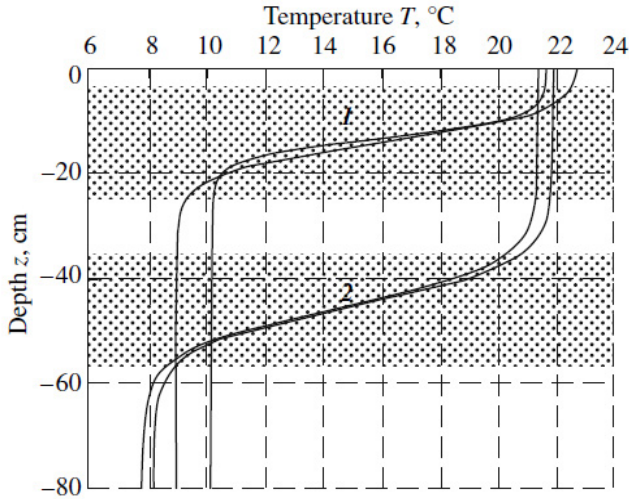


Fig. 2. Operating profiles of temperature stratification in the LTST. 1) shallow thermocline 2) deep thermocline. Two curves for each case indicates borders of stratification changing during experiments.

The scaled model of the diffuser of the sewer system was a metallic blanked-off tube at one end with the length of 1.3 m and the diameter  $d$  of 1.2 cm; the model includes 5 holes with the diameter of 3 mm located at a distance of 30 cm from each other at the same level. The tube is oriented horizontally across and in the middle of the tank (Fig. 1). The holes axes are oriented horizontally. The model is connected by a hose with a tank containing the solution of ethyl alcohol, the density of which during the experiments was kept constant ( $0.93 \text{ g/cm}^3$ ). Thus initial difference in density between jet and ambient fluid  $\Delta\rho_0$  was  $0.07 \text{ g/cm}^3$ . The outflow rate  $v_0$  from the diffuser model was: 40, 70, 100, and 150 cm/s (controlled by measuring the volumetric time rate). The variation of the flow rate through the change in the tank-solution level during the experiment does not exceed 10% (the average value was 5%).

The parameters of the induced jet flow and stratification in the LTST, enable us to simulate the typical conditions of the coastal area parameters of the submerged disposal system (Koh & Brooks, 1975) with respect to the  $Ri$ ,  $Str$  numbers (Bondur et al., 2009):

$$Ri = \frac{g\Delta\rho_0 d}{\rho_0 V_0^2} - \text{global Richardson number,}$$

$$Str = \frac{N_0^2 d \rho_0}{g\Delta\rho_0} - \text{parameter of ambient stratification,}$$

where  $\rho_0$  – mean density of ambient fluid,  $N_0$  – maximum buoyancy frequency of the ambient stratification,  $g$  – gravitational acceleration, and a geometric similarity on the scale of 1:27. In this case, the Reynolds number at the output was around 3000, which ensures the developed turbulence mode of buoyant jets in the laboratory experiment.

## 2.2 Measuring technique

Preliminary estimates indicated that the amplitudes of surface flows induced by internal waves would be only few mm/s. For these conditions, the modified Particle Tracking Velocimetry (PTV) method was used to measure the velocities of the surface flows induced by internal waves.

Thus, the limited area of basin surface under observation was seeded by particles of black polyethylene (density 0.98 g/cm<sup>3</sup>) with a characteristic size of about 1.5 mm for creating a contrast to the white background of the bottom (see the experimental setups in Figs. 1 a, b).

The motion of particles was recorded by a CCD camera from above (25 frames/sec), and the resulting time series of images were then processed on the computer. It turned out to be impossible to combine the particle observation region with the sensor allocation area (the distance between sensors and the observation area center is a minimum) in the conditions of this experiment, because the sensor images hindered the correct identification of particles on the images. That is why, two series of experiments were carried out with the sensors and the observation area allocated differently relative to the diffuser model.

The series *S1* (see Fig. 1 *a*) included the installation of 13 temperature sensors vertically at a distance of 200 cm from the diffuser model for measuring proprieties of internal waves; a scanning 3D ultrasound doppler anemometer (ADV) (at a distance of 260 cm); and the center of the observation area (at a distance of 400 cm), which is a 60×48 cm<sup>2</sup> rectangle was oriented by its longer side along the direction of the jet flow.

During the series *S2* (see Fig. 1 *b*), the surface observation area was located at a distance of 200 cm from the model. The area had dimensions 100×80 cm<sup>2</sup> and was oriented perpendicular to the flow motion. Further, at a distance of 300 cm from the collector model, temperature sensors were located and, at a distance of 360 cm, an ADV was located.

Two important problems concerning the measurements of surface flows in the LTST appeared during these experiments. The first one was that, when the temperature stratification with a shallow thermocline is created (Fig. 2), large-scale flows as a system of cyclonic and anticyclonic vortexes occurred on the surface layer. The measurements performed by the PTV method indicated that the scale of an individual vortex was 1.5–2.5 m, the maximum velocities of flows in it reached 1.3 cm/s, and the average velocities were about 4 mm/s. These values were calculated approximately, because the size of the observed area in both series of experiments did not allow one to cover the whole area at least one vortex. It can be assumed that vortexes appeared by inhomogeneous horizontal heating of the fine upper layer of thermocline. The presence of the large-scale flows made a low frequency trend in the dependence of the velocity on time, which was eliminated by the low frequency filtering of the results (see Subsection 2.3).

The second factor making it difficult to perform velocity measurements of surface flows is the presence of a Surface active substance (SAS) or dust film, which could not be completely removed.

We measured the parameters of the SAS film using the technique proposed in (Ermakov & Kijashko, 2006).

### 2.3 Modified algorithms of the PTV-method for studying weak surface flows

A classical PTV-method measures the velocity of each particle with respect to its motion on frames separated by a time interval and then reconstructs the velocity field by the velocity values at the points of the particle location. In these experiments, due to the presence of a background flow (see Subsection 2.2), the number of seeding particles in the observation area quickly decreased with time. For this reason we were able to determine only the averaged (over the observation area) value of the flow velocity. We found the trajectories of particles passing through this area and calculated their velocity at each moment. Then we calculated the velocity value averaged over all particles that were found in the observation area at the given time moment. The uncertainty of the PTV measurements was defined by the accuracy of the center of particle determination. It was about 10 % (based on results of special test experiments). To exclude the background low-frequency trends in the particle velocity, caused by large-scale flows in the LTST, we performed the low-frequency filtering of distributions of signals at frequencies below 0.02 Hz. The examples of such time dependences of the averaged surface flow velocity are shown in Fig. 3. These data were compared with oscillations of isotherms obtained from the temperature measurements (see Bondur et al., 2010 a).

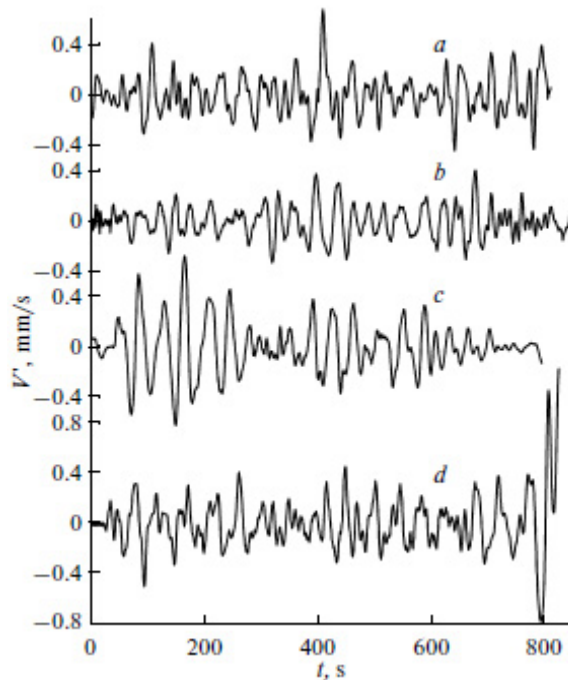


Fig. 3. Amplitudes of disturbances at the surface measured by the PTV method for rates of outflow from the diffuser model: *a*, 40 cm/s, *b*, 70 cm/s, *c*, 100 cm/s, and *d*, 150 cm/s.

## 2.4 Results - Comparing with theory forecasts

Basing on measured time realizations, we calculated the rms values of the surface velocity  $\langle V'^2 \rangle^{1/2}$ . The dependence of  $\langle V'^2 \rangle^{1/2}$  on the outflow rate from the diffuser model is shown in Fig. 4. It can be seen from here that  $\langle V'^2 \rangle^{1/2}$  varies in the range between 0.1 and 0.3 cm/s.

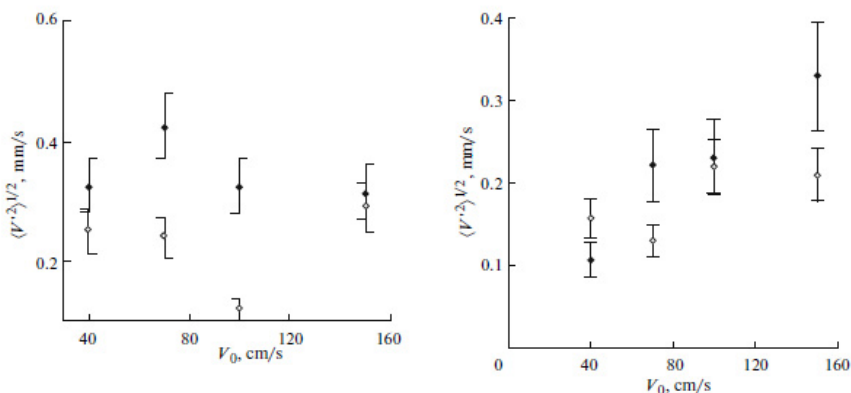


Fig. 4. Amplitudes of surface flow velocities (series S1 left and series S2 right): the black diamonds indicate theoretical estimates while accounting for the influence of the film and the light diamonds indicate the measurement results obtained by the PTV- method. Error bars corresponding to the uncertainty of the PTV measurements 10%, and uncertainty of theoretical estimations (determined by the accuracy of SAS films properties measurements 20 %).

The experimental data were compared with theoretical estimations of the value of the velocity on the surface according the theory of internal wave propagation proposed in (Bondur et al., 2010 a). Estimations were obtained taking into account the influence of the SAS films. The estimate for the error in theoretical values was determined by the measurement error (constituted 20%) (Ermakov & Kijashko, 2006). It is well seen from the figures that the results are in good agreement.

Thus, the experiments revealed that in the presence of internal waves induced by jets during outflow from the submerged sewer system model, surface flows with spatial periods controlled by the properties these waves appeared. The wavelength was from 30 to 160 cm. The standard deviations of velocities in the presence of a SAS film at the water surface varied in the range from 0.1 to 0.3 mm/s, corresponding to the amplitudes from 0.15 to 0.45 mm/s. For pure water the surface would constitute 1 to 2 mm/s. It should be pointed out that these experiments were performed for the conditions of scaled modeling.

In view of this, using the coefficients of scale modeling, one can estimate the flows created near the submerged sewer system in nature conditions: the parameters of internal waves (induced by jets), and the prosperities of their surface manifestations, as well as make conclusions on the possibility of remote diagnostics of these waves. In our laboratory experiment the coefficient of scale modeling with respect to the velocity value constitutes 1.3 and the coefficient of

geometric similarity was 1:27. In view of this, we revealed the fact that this experiment simulated stratification with a pycnocline thickness of about 4 m, an internal wave with the length from 8 to 43 m, celerity from 5 to 10 cm/s, and the surface flow velocity from 0.3 to 0.6 cm/s. For such flows it yielded an estimate (see (Bondur et al., 2010 b)) for the contrast in the field of short waves of 0.12–0.3, which can be confidently detected by modern remote sensing methods (Bondur, 2004, 2006, 2011; Bondur, Grebenuyk, 2001).

### 3. The experimental study of the interaction of buoyant turbulent jet with pycnocline stratification with the PIV-method

A theory describing the relation of characteristics of surface manifestations with the operational parameters of sewer systems should be made. For this propose it is necessary to investigate the dynamics of the buoyant jets in the pycnocline region, where the trapping of the jets by stratification occurred. The PIV-method is widely used for studying the velocity fields of the jet flows. However, there are several problems of carrying out measurements by PIV-methods in LTST (see Section 4). That is why preliminary test experiments of applying PIV-methods were provided in a small reservoir with saline stratification.

#### 3.1 Experimental setup in saline stratification

To study the properties of the buoyant turbulent jets and ambient stratified liquid interaction, we performed preliminary test experiments in a small plexiglas basin with saline stratification. The scheme of the experiment is shown in Fig.5.

Here, a salt stratification of the pycnocline type is created. The distributions of density and buoyancy frequency are shown in Fig. 6.

In this experiment, the diffuser model had only a single vent with a diameter of 1.2 mm that allowed fresh water to flow out with the rate of 50 cm/s and form buoyant jet in ambient salt water.

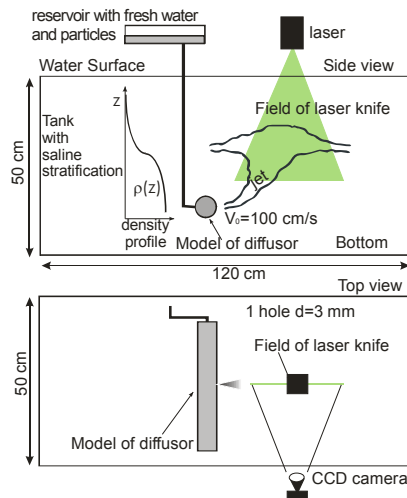


Fig. 5. Principal scheme of experimental setup.



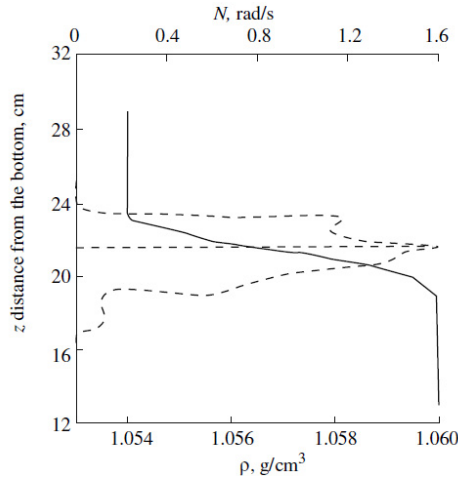


Fig. 6. Distributions of density (solid line) and buoyancy frequency  $N = \sqrt{\frac{g}{\rho} \frac{d\rho}{dz}}$  (dashed line) in the small reservoir.

The PIV method was used to study the jet flow. Polyamide particles 50  $\mu\text{m}$  were added to the reservoir with freshwater. We put particles only in the jet, because we want to see and measure the form and boundary of the jet precisely (oscillations of the top of the jet). The motion of particles in the jet was visualized by a vertical laser sheet along the jet axis. The source - CW NdYag laser (532 nm wavelength, 0.5 Wt power). The lateral view was recorded on a CCD-camera (example of the buoyant plume is shown in Fig. 7) with the rate of 25 frames per second and exposure time of 5 ms. The displacement was less than 1 pxl during time exposure.

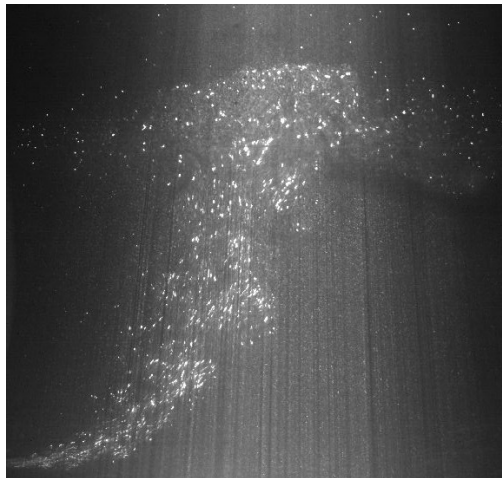


Fig. 7. Example of the buoyant plume.

### 3.2 PIV-processing

The main attention was drawn to the area of the front of the fountain. The processing of the resulting frame sequences by PIV algorithms made it possible to obtain the velocity field in the laser-sheet cross section at consecutive time points with a step of 0.25 s by the way of cross correlation processing successive pairs of frames. The interrogation window size was  $32 \times 32$  pix, with 50 % overlapping. The Gaussian approximation of the correlation function was used to avoid the effect of peak locking. The measurements uncertainty by PIV-method was about 3 %. It was obtained from the processing of synthetic images with determined displacement. Fig. 8 shows examples of measured instantaneous velocity fields.

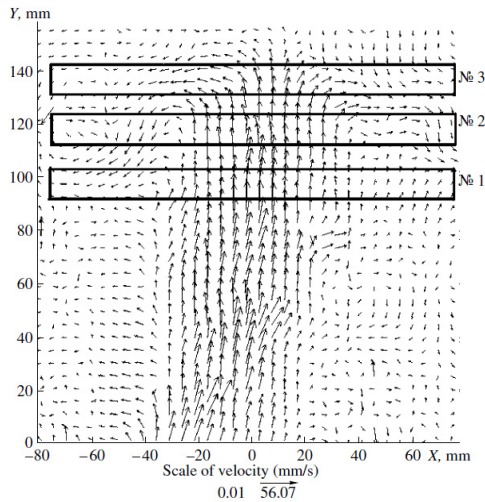


Fig. 8. Velocity field of buoyant turbulent jet.

It can be clearly seen that the jet is trapped by the stratification and propagates at the neutral buoyancy level, which is located on the lower boundary of the pycnocline. The video recording also indicated that the upper boundary of the jet oscillates in the vertical plane; the oscillation spectrum of the front clearly expressed peak at a frequency of 0.1 Hz (Fig. 9).

### 3.3 Main results of the experiment

Fig. 10 shows the instantaneous velocity profiles in different cross sections of the jet. To smooth the turbulent fluctuations that arise on these profiles, averaging by the coordinate along the jet axis over three domains shown in Fig. 8 was used. This includes the calculation of the mean profile of velocity on the basis of three adjacent profiles located 4.8 mm away from each another. It can be seen from the Fig. 10 that the counterflow exists in the region of pycnocline.

A stability analysis for the resulting profiles of flow velocities performed by the method of normal modes has revealed that, for the jet with the counterflow region, the condition of absolute instability by the Briggs criterion (Briggs, 1964) for axisymmetric jet oscillations is satisfied. The stability of nonparallel currents is normally analyzed in the following way: the

current is divided into parts, each of which is taken to be quasi-parallel and treated by the method of normal modes. It testifies to the fact that the globally unstable mode (Monkewitz et al., 1993) is actuated. The estimates for oscillation frequencies of the globally unstable mode are well consistent quantitatively with the measured spectrum of jet oscillations (see. Fig 9).

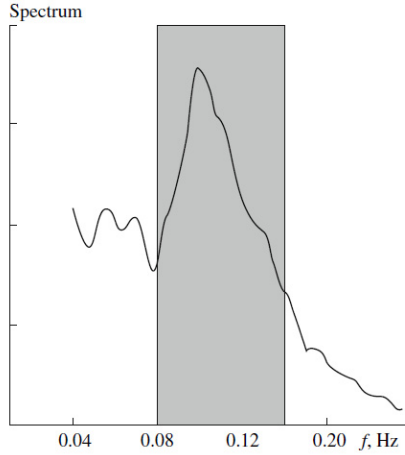


Fig. 9. Spectrum of oscillations of the upper boundary of the jet, the gray field indicates boundaries of theoretically predicted frequency of oscillations basing on the stability analysis (semi-logarithmic scale)

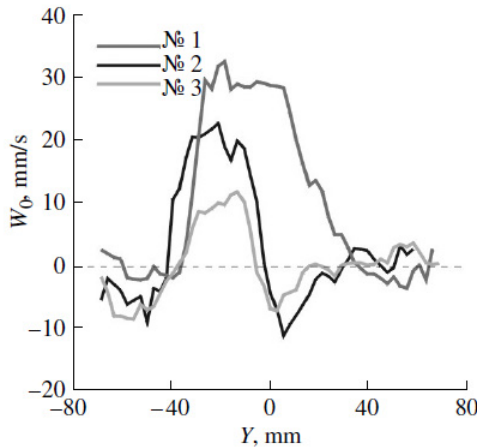


Fig. 10. Profiles of jet rate in cross sections 1, 2, and 3 (see Fig. 8).

Thus, the following mechanism of internal wave generation by buoyant plume is proposed. (Huerre et al., 1990). Self induced oscillations of the globally unstable mode appear during the interaction of a buoyant plume with the pycnocline. Internal waves are intensely generated if the frequency of these oscillations turns out to be lower than the maximal buoyancy frequency in the pycnocline.

#### 4. Investigation of the mechanisms of internal waves generation by buoyant jets within the laboratory modeling of submerged sewage in a stratified ocean with the PIV-methods

Basing on the results of successful applying of the PIV-methods in small reservoir with saline stratification a series of similar experiments in the LTST for the conditions of scale modeling of the typical sewer system (see Section 2) were carried out for approving the hypothesis offered in section 3. In these experiments for the first time simultaneous measurements of the jet characteristics (source of oscillations) with PIV-method and the properties of internal waves by contact methods were performed.

##### 4.1 Experiments in LTST with the application of the PIV-technique

The simplified general experimental scheme is shown in Fig. 11. This scheme is similar to the one we used for the experimental investigation of surface flows (see Section 2). In this experimental series the temperature stratification was created in LTST with the thermocline center located at the depth of 43-45 cm. Full water depth in the Tank was 160 cm (profile 2 in Fig. 2).

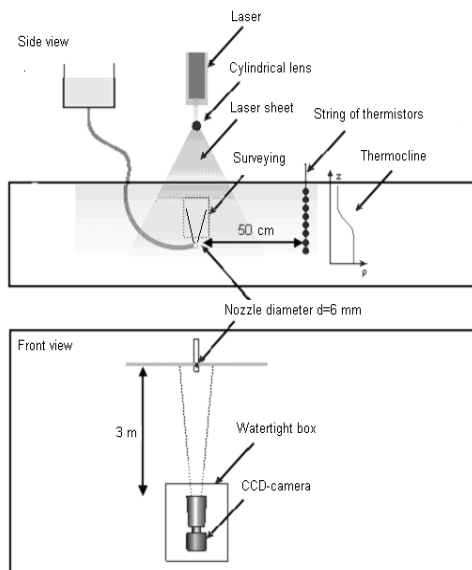


Fig. 11. Experimental setup: visualization of a turbulent jet in LTST

Opposite to the previous experimental series in LTST (see Section 2), a jet was discharged vertically from a  $\Pi$ -shaped round pipe of 6 mm diameter (see Fig. 11), i.e. only one nozzle was used. Previously we worked with several buoyant jets (alcohol solution) discharged horizontally from a diffuser model at different rates.

The laboratory modeling of the jets from disposal systems showed that jets do not merge until they reach pycnocline. The visualization of such flows and the application of the PIV-

technique in LTST were a very complicated task. Horizontally discharged buoyant jet comes to the pycnocline nearly vertically at some distance from the nozzle (see the jet photo from the experiment in Fig. 7, and calculations result in Fig. 12). In order to perform successful jet-thermocline interaction survey of a high space resolution we have to know this distance with a very high accuracy just to place the camera and the laser system correctly. It should be noted, that this distance depends strongly on a jet flow rate resulting in difficulties with equipment positioning

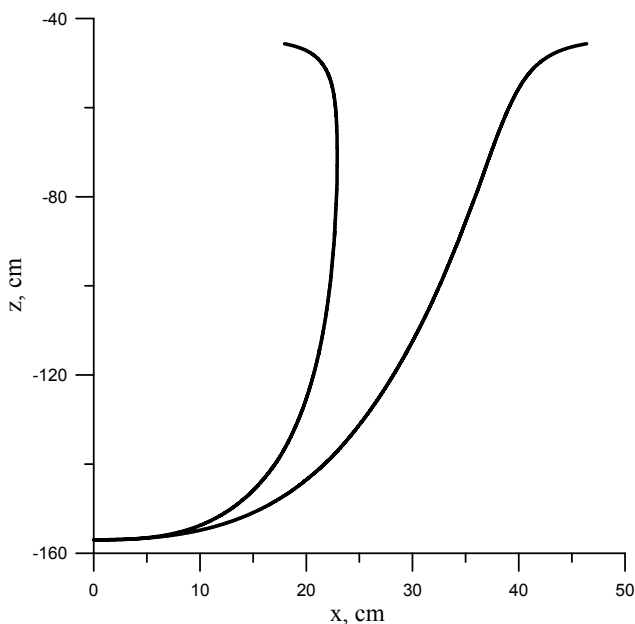


Fig. 12. Jet trajectory (boundaries) calculated for typical stratification in LTST basing on the integral model (thermocline center is at 44 cm depth). Side view.

Alcohol solutions also cause problems for visualization (chemical interaction with polyamide particles). Thus, in the new experimental series we used one jet of neutral buoyancy, discharged vertically at several rates. Jet exit velocity and a distance from the nozzle to the thermocline were chosen to provide jet parameters in the thermocline coincident with those in the previous series on the laboratory scale modeling of sewage disposal systems (see Section 2). Jet parameters in the thermocline for the series with buoyant liquid were determined from the direct numerical solutions to the system of equations for integral parameters of a turbulent jet in ideal incompressible liquid (Fan 1968).

New series consisted of 10 experiments: 2 for each flow rate. Jet parameters in the thermocline measured experimentally are shown in Fig.13.

Velocity fields in a jet were studied by the PIV-method. For jet visualization  $20\ \mu\text{m}$  polyamide particles were added to jet liquid. Only jet was seeded, for precise measurements of boundary oscillations. Particles were put to a reservoir 5 minutes after the beginning of each experiment. The laser sheet was produced by the same laser we used in the previous

experimental series. Since LTST walls are not transparent, the digital camera (frame rate 25 frames/sec, time exposure 10 ms) was placed into a specially designed waterproof box (we performed underwater survey). The time exposure was 2 ms. Displacement of the particles less 1 pxl during one frame. The camera was submerged to the thermocline level at the distance 3 m from the nozzle (a maximum possible distance). The digital data from the camera were processed out with "Vortex" program which was also used previously to calculate the velocity fields, and a specially developed "SMPD" algorithm for simultaneous work with the survey data and calculated velocity fields.

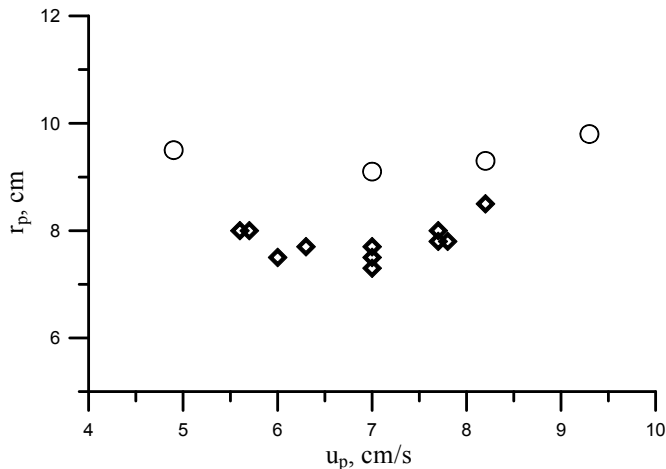


Fig. 13. Experimental jet parameters (maximum longitudinal velocity and radius): O – calculated in the framework of the integral model for discharge rates of buoyant jets 40, 70, 100 and 150 cm/s;  $\diamond$  - parameters, measured in the experiments with one jet.

Temperature oscillations in the LTST during jet discharge were measured as in previous experiments by contact methods (a string of 13 thermistors was employed). The string was placed at 50 cm distance from the nozzle. Using the data from thermistors we calculated isotherms.

The underwater survey in each experiment lasted 20 min (during this time particles were added to the reservoir from time to time) and temperature oscillations were measured during the whole time of the experiment – 1 h.

#### 4.2 Processing technique for video and velocity fields

We studied jet oscillations in the thermocline using the SMPD algorithm. It allows calculating the average intensity of a frame in the user-defined rectangular area, thus, intensity dependence on time can be easily derived. If a rectangular area is chosen in the jet oscillations region, the intensity dependence detects these oscillations due to the light particles in the jet. We also employed the next considerations when chose the area. One could expect 2 types of unstable jet modes to develop: the first was axisymmetric and the second was spiral or helical. An axisymmetric mode results in the jet top oscillations in the vertical plane, and a spiral one in the laser sheet plane looks like jet oscillations from left to right. In order to detect both

modes, one rectangular side was chosen along the jet axis and the other side separated the area with particles from the rest, simply black area (see Fig. 14). Upper and bottom rectangular sides indicated the maximum and minimum jet top positions. Jet top oscillations were calculated for each experiment (an example is shown in Fig. 15a).

It should be noted, however, that particles concentration in a jet changed in time causing changes in average intensity. This resulted in the average intensity trend. At the moments of particles injection in the reservoir one could observe sudden changes of intensity. Besides, slow intensity decrease due to decreasing particles concentration could also lead to incorrect ratio of power spectral peaks, and oscillations corresponding to the film beginning or particles injection moments would be the most powerful.

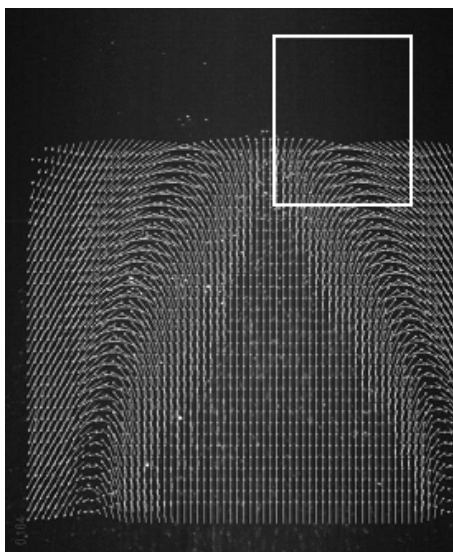


Fig. 14. An example of rectangular area for investigation of jet top oscillations. Mean velocity field is calculated on the PIV-measurements base.

Thus, the calculated intensity had to be corrected. For each experiment we found the intensity trend due to varying particles concentration in a jet. This was performed by choosing a maximum possible rectangular area in a jet fully occupied by particles and calculating its average intensity dependency on time (Fig.15 b). The bigger this area is, the smaller high-frequency pulsations of intensity are. Jet top oscillations can be represented by a formula

$$y(t)=I(t)*f(t),$$

where  $f(t)$  - is jet oscillations function, as it would be for the constant particles density;  $I(t)$ - function, corresponding to the average intensity trend (or particles concentration trend).

Then a desired function is  $f(t)=y(t)/I(t)$  (see example in Fig. 15 c). When processing data out, high-frequency oscillations were filtered from  $I(t)$ .

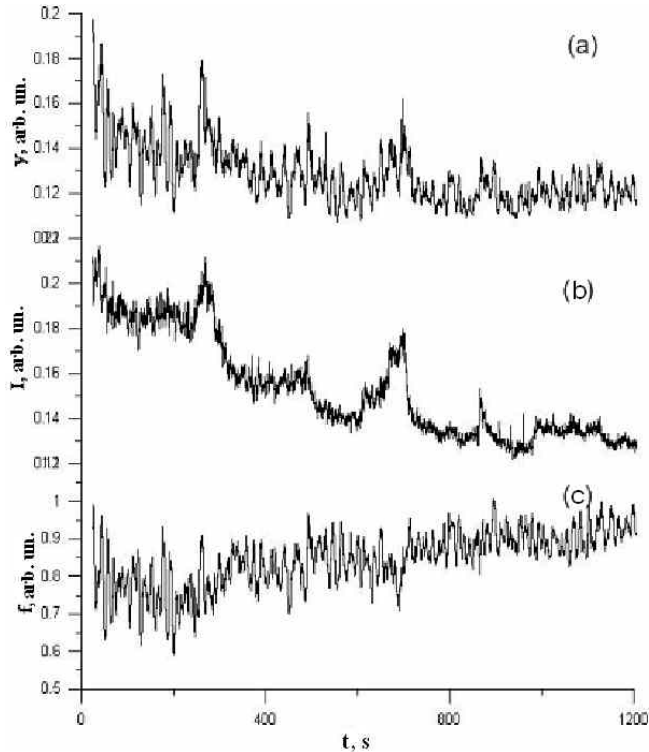


Fig. 15. Average intensity oscillations of the digital image (the gradations of grey color - 12 bit) (a), intensity change due to varying particles concentration (b); jet top oscillations (c). All taken from rectangular area in Fig 14

### 4.3 Experimental results. The comparison between internal waves and jet top oscillations spectra

During the experiments the turbulent jet, as in previous series, spread at the level of neutral buoyancy, forming a horizontal shear flow under the thermocline, and generated intensive internal waves. We calculated internal waves spectra for all experiments and revealed pronounced peaks in the frequency interval between  $f_{min}=0.02$  Hz и  $f_{max}=0.05$  Hz, with maximum buoyancy frequency being 0.07 Hz.

Jet top oscillations spectra (spectra of functions  $f(t)$ ) were found for all experiments and compared to spectra of isotherms  $T=16^{\circ}\text{C}$ , close to the thermocline center (from the 1h realization we cut 20 min corresponding to survey time). The examples of such spectra are shown in Fig. 16 for experiment with discharge rate 150 cm/s. There exists a pronounced peak at the frequency close to  $0.7N_0$  in the internal waves spectrum. It can be seen from the figure, that jet oscillations at frequency  $0.7N_0$  generate internal waves most effectively. Theoretical analysis performed basing on the work [Bondur et al, 2010a] for source parameters taken from our experiments confirms the most effective generation of internal waves at this particular frequency.



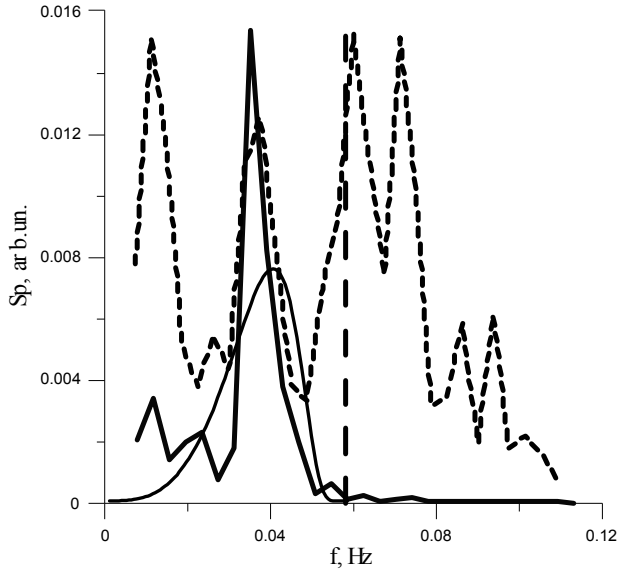


Fig. 16 Jet top oscillations spectrum (hatch line) and spectrum of isotherm (solid line), corresponding to the thermocline center for the experiment with discharge rate 150 cm/s. The straight line marks the maximum buoyancy frequency. The smooth curve is a frequency dependence of the internal waves excitation coefficient.

#### 4.4 Jet mode structure investigation with the application of the PIV-method

In this Subsection we determine an unstable jet mode type generating internal waves. For this purpose we used a modified method, developed in (Yoda et al., 1992), where the jet mode structure was investigated basing on the experimental data for a turbulent round jet at a distance  $x/d \gg 1$  ( $x$  is a distance from the nozzle,  $d$  is a nozzle diameter). The method is based on cross-correlation processing of the digital survey data. First, in each frame from the film jet boundaries were determined – areas of the same intensity defined by the authors. Then for several jet cross sections they obtained jet boundaries dependencies on time (2 for every cross section) and calculated their cross-correlations. Basing on these data, a prevailing jet mode was determined.

Let's illustrate this method application on the example. Let the axisymmetric jet mode dominate. Jet boundaries dependencies for this case are shown in Fig. 17. If one of them is reflected with respect to the jet axis, the curves  $a$  and  $b$  coincide. Their cross correlation function is periodic and has a maximum in zero. If a spiral mode prevails (Fig. 17), the function has a minimum at  $t=0$ .

We modified this method: jet boundaries were determined using longitudinal jet velocity profiles, calculated by means of the PIV-method. In order to reduce high-frequency fluctuations, we averaged velocity fields by time and coordinate along the jet axis. The averaging time and length were chosen small as compared to characteristic time and spatial scales. Characteristic time corresponding to the frequency  $0.7N_0$  was 25 s. The averaging

time was  $t_{avg} = 2c$ . The wavelength of the unstable jet mode had to be of jet diameter order, which was 15-16 cm in the thermocline. Thus, 5 neighbour jet velocity profiles were averaged, located at a distance 1 cm from each other and the average length was, consequently,  $l_{avg} = 4$  cm (see Fig. 18).

For each experimental frame sequence consisting of 30000 frames, 5 rectangular areas were chosen, as a rule, 2 of them were in thermocline, 2 - above it and 1 - below (see Fig. 18). For each rectangular area the SMPD algorithm was employed to make a file containing averaged by  $t_{avg}$  and  $l_{avg}$  longitudinal velocity profiles for successive time moments at interval  $t_{avg}$ . Using these data we obtained the maximum velocity and jet boundaries dependencies on time for each rectangular area. Jet boundaries were determined by  $e$  times velocity decrease from the maximal meaning.

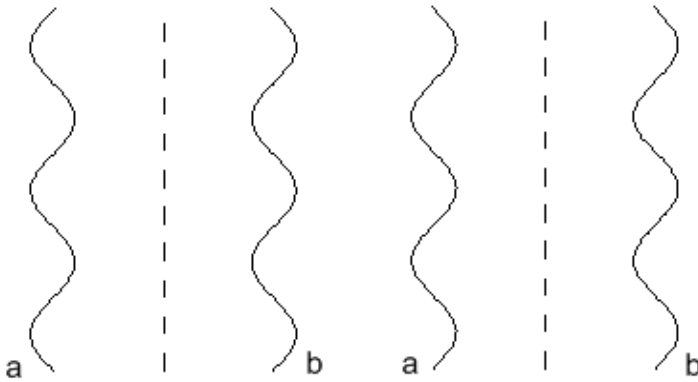


Fig. 17. Jet boundary dependencies on time for some jet cross-section: left - axisymmetric mode, right - spiral mode.

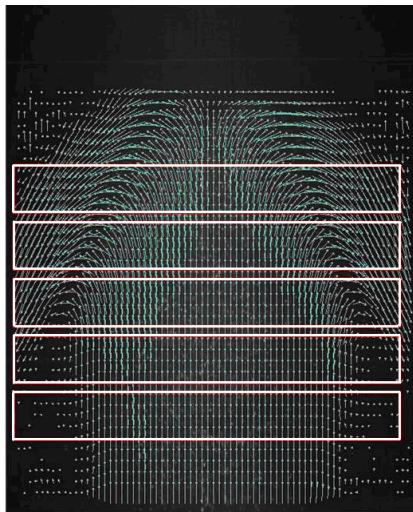


Fig. 18. An example of rectangular areas for velocity profiles averaging

In order to determine a mode, generating internal waves, every jet boundaries function was filtered with cut-off frequencies 0.02 Hz and 0.05 Hz. For each rectangular area we calculated jet boundaries cross-correlation functions, see Fig. 19 as an example. It can be seen from this figure, that functions has maxima at  $t = 0$ , consequently, the axisymmetric mode prevails at generation frequency of internal waves.

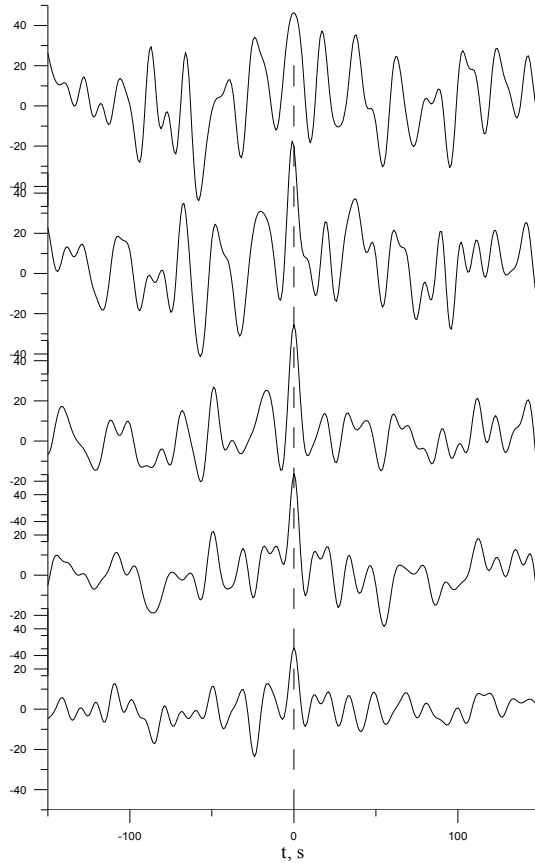


Fig. 19. Example of cross-correlation functions of jet boundaries for 5 rectangular areas in Fig. 18 in the same order – experiment with discharge rate 150 cm/s.

## 5. Conclusion

Investigation of hydrodynamic processes near submerged wastewater outfalls is an important scientific and engineering problem. Method of dye colouring for jet visualization has been extensively used both in laboratory and field conditions. It allowed observing and investigating evolution of jet integral parameters, in particular, jet spread and dilution laws, oscillations of buoyant jet fronts, both in homogeneous and stratified liquid. At the same time, precise and very specific experiments were needed to clarify the possibility of surface manifestations of the jets from submerged wastewater outfalls. This task demanded

measurements of velocity fields of surface flows and in water column with high time and spatial resolution. Thus, optical PIV/PTV methods were optimal. This Chapter is devoted to application of these methods for investigation of dynamics of flows from submerged wastewater outfalls and their surface manifestations.

For this purpose a physical scale modeling of internal waves generation by the turbulent buoyant jets induced by submerged sewer in conditions of temperature stratification with shallow thermocline in LTST IAP RAS was performed. Velocity fields of the surface flows induced by internal waves were measured by the modified PTV-method. The modified method allowed to identify these very weak surface flows in the presence of large-scale background flows. The obtained experimental data are in good agreement with theoretical forecasts taking into account presence of a SAS film, which could not be eliminated completely. For the known parameters of the film and coefficients of scale modeling, we estimated the parameters of internal waves generated by a submerged sewer jet flows and the values of their surface manifestations for the nature conditions. The estimations of hydrodynamic contrasts (caused by manifestations) in the field of surface waves obtained in [Bondur 2004, 2006, 2011, Bondur & Grebenyuk 2001], show that such contrast could be detected with confidence by the modern remote sensing methods.

The experiments on measurements of submerged flows with PIV-methods were carried out for the purpose of studying mechanisms of internal waves generation by buoyant jets. At first preliminary test experiments were performed in small reservoir with saline stratification. It turned out that, when the jet approaches the pycnocline, a counterflow is generated at the edges. A stability analysis for the resulting profiles of flow velocities performed by the method of normal modes has revealed that, for the jet portions with counterflow, the condition of absolute instability criterion for axisymmetric jet oscillations is satisfied. The estimates for oscillation frequencies of the globally unstable mode are in good agreement with measured spectrum of the jet oscillations.

These experiments were continued as a laboratory scale modeling of submerged wastewater outfalls in LTST with application of PIV-technique for measurements of jets' parameters and contact methods for investigation of internal waves. It allowed to compare jet oscillations spectra, obtained by modified video images processing, with spectra of internal waves. The comparison confirmed that self-sustained jet oscillations serve as a source of internal waves. The investigation of mode structure of jet perturbations with application of modified PIV-method showed that the axisymmetric mode prevails and it effectively generates internal waves.

Within the framework of this study modified methods of using PIV/PTV technique were developed for the complicated investigations of turbulent submerged flows and its surface manifestations in the conditions of ambient stratification together with contact methods.

## 6. References

- Adrian, R. J., (1991) Particle Imaging techniques for experimental fluid mechanics. *Annu. Rev. Fluid Mech.*, Vol. 23, p. 261–304.
- Arabadzhi, V. V., Bogatyrev, S. D., Bakhanov, V. V, et al (1999) Laboratory Modeling of Hydrophysical processes in the Upper Ocean Layer (Large Thermostratified Tank

- Institute of Applied Physics, Russian Academy of Sciences), in *Near-Surface Ocean Layer. Physical Processes of Remote Probing*, V. I. Talanov and E. N. Pelinovskii, Vol. 2, pp. 231–251, IAP RAS Press, Nizhni Novgorod, [in Russian].
- Beckers, M.R., Clercx, H., Heijst van G.J.F. & Verzicco, H.J.H. (2003) Evolution and instability of monopolar vortices in a stratified fluid. *Phys. Fluids*, Vol. 15, pp. 1033–1045.
- Bondur V. G., (2004) Aerospace Methods in Modern Oceanology, in *New Ideas in Oceanology, Vol. 1: Physics. Chemistry. Biology*, pp. 55–117, Nauka Press, Moscow, [in Russian].
- Bondur, V., (2006) Complex Satellite Monitoring of Coastal Water Areas *Proceedings of 31st International Symposium on Remote Sensing of Environment, ISRSE*, pp. 31 – 35.
- Bondur, V.G. (2011) Satellite monitoring and mathematical modelling of deep runoff turbulent jets in coastal water areas In *Waste Water*. <http://www.intechopen.com/articles/show/title/satellite-monitoring-and-mathematical-modelling-of-deep-runoff-turbulent-jets-in-coastal-water-areas>, pp. 26–32, Intech.
- Bondur, V. G. and Grebenyuk, Yu. V., (2001) Remote Indication of Anthropogenic Impacts on the Marine Environment Caused by Deep-Water Sewage Discharge *Issl. Zemli Kosmosa*, No. 6, pp. 1–12 [in Russian].
- Bondur. V., Tsidilina M. (2006) Features of Formation of Remote Sensing and Sea truth Databases for The Monitoring of Anthropogenic Impact on Ecosystems of Coastal Water Areas. *Proceedings of 31st International Symposium on Remote Sensing of Environment, ISRSE*, pp. 192–195.
- Bondur V., Keeler R., Gibson C. (2005) Optical satellite imagery detection of internal wave effects from a submerged turbulent outfall in the stratified ocean *GRL*, 32, L12610, doi:10.1029/2005GL022390.
- Bondur, V. G., Zhurbas, V. M., and Grebenyuk, Yu. V. (2006), Mathematical Modeling of Turbulent Jets of Deep- Water Sewage Discharge into Coastal Basins, *Oceanology*, Vol. 46, No. 6, pp. 757–771.
- Bondur, V.G., Zhurbas, V.M., Grebenuk Yu.V. (2009) Modeling and Experimental Research of Turbulent Jet Propagation in the Stratified Environment of Coastal Water Areas *Oceanology*, Vol. 49, No. 5, pp. 595–606.
- Bondur V.G., Grebenyuk Yu.V., Ezhova E.V., Kazakov V.I., Sergeev D.A., Soustova I.A. and Troitskaya Yu.I. (2009) Surface Manifestations of Internal Waves Investigated by a Subsurface Buoyant Jet: 1. The Mechanism of Internal-Wave Generation *Izvestiya, Atmospheric and Oceanic Physics*: Vol. 45, No 6, pp. 779–790.
- Bondur V.G., Grebenyuk Yu.V., Ezhova E.V., Kazakov V.I., Sergeev D.A., Soustova I.A. and Troitskaya Yu.I. (2010) Surface Manifestations of Internal Waves Investigated by a Subsurface Buoyant Jet: 2. Internal Wave Field *Izvestiya, Atmospheric and Oceanic Physics*: Vol. 46, pp. 768 - 779.
- Bondur V.G., Grebenyuk Yu.V., Ezhova E.V., Kazakov V.I., Sergeev D.A., Soustova I.A. and Troitskaya Yu.I. (2010) Surface Manifestations of Internal Waves Investigated by a Subsurface Buoyant Jet: 3. Surface Manifestations of Internal Waves *Izvestiya, Atmospheric and Oceanic Physics*: Vol. 46, No. 4, pp. 482–491.
- Briggs, R. J. (1964) *Electron-Stream Interaction with Plasmas* MIT Press, Cambridge.
- Ermakov, S.A., Kijashko, S.V. (2006). Laboratory study of the damping of parametric ripples due to surfactant films In *Marine surface films*. pp.113–128. Springer. Germany.

- Fan, L.N. (1968) Turbulent buoyant jet problems. In *Rep. No. KH-R-18* Calif. Inst. Technol.USA.
- Gibson C.H., Bondur V.G., Keeler R.N., Leung P.T. Energetics of the Beamed Zombie Turbulence Maser Action Mechanism for Remote Detection of Submerged Oceanic Turbulence. *Journal of Applied Fluid Mechanics*, Vol. 1, No. 1, pp. 11-42, 2006.
- Gibson C.H., Bondur V.G., Keeler R.N., Leung P.T. Remote sensing of submerged oceanic turbulence and fossil turbulence. *International Journal of Dynamics of Fluids*, Vol.2, No.2 (2006), pp. 171-212.
- Gibson C.H., Keeler R.N., Bondur V.G. (2007) Vertical stratified turbulent transport mechanism indicated by remote sensing. *Proceedings of SPIE, Coastal Remote Sensing*. SPIE Newsroom, Vol. 6680. 26-27 Aug.
- Gibson, C.H., Bondur, V.G., Keeler, R.N., Leung, P.T., Prandke, H., Vithanage, D. (2007). Submerged turbulence detection with optical satellites, *Proceedings of SPIE, Coastal Remote Sensing*. SPIE, Vol. 6680, 6680X1-8. doi: 10.1117/12.732257 Aug. 26-27 2007
- Heijst van G.J.F., Beckers, M., R. Verzicco, H.J.H. (2002) Dynamics of pancake-like vortices in a stratified fluid: experiments, model and numerical simulations. *Journal Fluid Mech*, Vol. 433, pp. 1-27.
- Koh, C.Y. and Brooks, H.N. (1975) Fluid mechanics of waste-water disposal in the ocean *Annu .Rev. Fluid Mech*, Vol. 8, pp.187-211.
- Monkewitz, P. A., Huerre P., Chomaz J.-M., (1993) Global Linear Stability Analysis of Weakly Non-Parallel Shear Flows, *J. Fluid Mech*. Vol. 251, pp. 1–20.
- Ozmidov R. V., (1986) Diffusion of Admixture in the Ocean. Gidrometeoizdat, Leningrad, [in Russian].
- Reul, N., Branger, H., Giovanangeli, J.P. (1999) Air flow separation over unsteady breaking waves *Phys. Fluids*. Vol. 11. pp. 1959–1961.
- Sergeev, D.A., Troitskaya, Yu.I., (2011) APPLYING OF PIV/PTV-methods in Laboratory modeling of geophysical flows In *Modern optical methods of flows investigations* Ed. Rinkavichus B.S. pp. 330-347, Overley Press. Moscow.
- Troitskaya, Yu. I. , Sergeev, D. A., Ezhova, E. V., Soustova, I. A., and Kazakov, V. I. (2008) Self-Induced Internal Waves Excited by Buoyant Plumes in a Stratified Tank, *Doklady Earth Sciences*, Vol. 419A, pp. 506 -510.
- Turner, J. S. (1966) Jets and plumes with negative or reversing buoyancy *Journal Fluid. Mech.*, Vol. 26, p. 779-792.
- Umeyama M., (2008) PIV Techniques for Velocity Fields of Internal Waves over a Slowly Varying Bottom Topography *Journal of Waterway Port Coastal and Ocean Engineering* Vol. 134, No. 5, pp. 286-298.
- Veron, F., Saxena, G., Misra, S.K. (2007) Measurements of the viscous tangential stress in the airflow above wind waves *Geophys. Res. Lett.*, Vol. 34, L19603. doi: 10.1029/2007GL031242.
- Zhang H. P., King B., and Harry L. Swinney Experimental study of internal gravity waves generated by supercritical Topography // *Physics of Fluids* (2007) 19, 096602
- Yoda M., Hesselink L., Mungal M.D. The evolution and nature of large-scale structures in the turbulent jet // *Phys Fluids A*. 1992. V.4. No.4. P. 803-811.